

# Toward Sentient Neurotechnology

## *Visual Object Unity May Be Structured by and Constrain Neural Interactions*

Raymond Pavloski

*Psychology Department, Indiana Univ. of PA, 15701, Indiana, PA, U.S.A.*

**Keywords:** Hard Problem, Neurotechnology, Recurrent Neural Network, Sentience, Tolerance Space, Visual Object Unity.

**Abstract:** Achieving an understanding of how qualities of experience arise in concert with the operation of neural networks could produce a revolutionary advance in neurotechnology. The work reported here explores a relationship between a visual quality and neural activity that has not previously been investigated: visual object unity may emerge from and constrain neural interactions. Simulations were employed to determine if a topological signature of a unified object develops as a recurrent neural network's activity is modulated by retinal input. Results show that differences in recurrent excitatory conductance values produced by adjacent active neurons are negligibly small, and can be described by a tolerance relation. Tolerance open balls about the vectors of conductance values produced by active neurons emerge in response to the retinal image of an object and a connected open set consisting of intersecting open balls quickly develops. Such connected open sets are invariant over fluctuations in participating neurons, demonstrate several characteristics of perception, and are hypothesized to be objective signatures of perceived object unity. Dynamical network phenomena, such as hysteresis, lead to empirical predictions that can be tested with human participants. Means of identifying objective signatures in brain activity are considered.

## 1 INTRODUCTION

The domain of neurotechnology is limited by the absence of an explanation for how the qualities of experience arise in concert with the operation of neural networks in the brain, often referred to as the 'hard problem' (Chalmers, 1996; Hut and Shepard, 1996). As a result of this limitation, we are unable to construct a cortical prosthesis that when interfaced with damaged visual cortex would make it possible for a patient to regain aspects of visual experience that have been lost through cortical lesions.

There is no doubt that significant progress has been made in identifying objective signatures of conscious access, the ability to report an experience following presentation of a stimulus (Dehaene, 2014). However, this achievement provides no information regarding the neural mechanisms involved in the appearance of a particular quality of experience (Block, 2001; 2007). Nor does it provide any information on how the processes that underlie any specific quality of experience are involved in neural dynamics. Without such information, it is difficult to take seriously the claim that "there is now sufficient evidence to consider the design and construction of a

conscious artifact (Edelman et al., 2011)."

It seems unlikely that a general solution to the hard problem will be found in the absence of work that relates specific aspects of experience to specific aspects of neural activity. In order for experimental and theoretical progress to be made, it is essential that an aspect of experience can be described so that its relation to neural activity is evident. This report puts forward the appearance of visual object unity (Chen, 2005), modelled as a connected open set in a tolerance space (Peters and Wasilewski, 2012), as such an aspect of experience.

From a naïve viewpoint, it is easy to overlook the fact that the experience of a unified entity, one aspect of the full experience of a visual object, is an achievement of the visual system. Of course, this is obvious to those who believe that vision proceeds from part to whole and from geometrically simple to geometrically complex. From this perspective, it is assumed that receptive field data show that an object image is initially decomposed into patches of contrast, and that processes in successively higher cortical areas in some way bind successively more complex geometric features into the visual object that is experienced (e.g., Roelfsema and Houtkamp,

2011). The topological approach to perceptual organization that is advanced by Chen (2005; see also Zhang, 2005) is in agreement with the conclusion that visual object unity is an achievement of the visual system. According to this approach, however, visual unity is a topological visual primitive and is extracted from the object image very early in visual processing.

Despite the volume of excellent experimental work carried out by Chen and his colleagues in support of the topological approach, the means by which visual neural networks deal with topological properties has remained a mystery (Minsky and Papert, 1988; Pomerantz, 2003). As indicated by Chen (2005), the topological approach can be made compatible with the fundamentally discrete nature of the visual system if it is assumed that vision is tolerant to differences in the retinal image at various scales. For example, visual unity can readily be perceived in a collection of image elements that are spatially separated by sufficiently small distances. This is expressed formally by stating that a pair of image elements belongs to a tolerance relation  $\tau$  if the distance between them is less than some criterion. Like equality, tolerance  $\tau$  is a relation that is reflexive (for an element  $a$ , the pair  $(a,a)$  belongs to  $\tau$ ) and symmetric (if  $(a,b)$  belongs to  $\tau$ , then  $(b,a)$  belongs to  $\tau$ ). Unlike equality, however, tolerance is not transitive:  $(a,b)$  belongs to  $\tau$  and  $(b,c)$  belongs to  $\tau$  do not imply that  $(a,c)$  belongs to  $\tau$ . Work in computational vision shows that it is possible to apply a tolerance relation to the elements of an image and thereby to identify topological properties of the image (Huang et al., 2010). How the brain might accomplish this task is not known. More importantly, even having a neural network that computes topological properties might not tell us how the experience of visual unity arises within that network, how we *see* visual unity.

An alternative approach is to study the sources and consequences of a tolerance relation within the recurrent neural interactions of richly interconnected networks of the visual system. Introducing a bit of tolerance space terminology is very helpful in seeing how this might be done (Peters and Wasilewski, 2012). If we use accepted terminology, then the set of elements  $x$  such that  $(a,x)$  belongs to  $\tau$  is called an open ball about  $a$ , or  $OB(a)$ . For example, we might have  $OB(a) = \{a,b\}$ ,  $OB(b) = \{a,b,c\}$ , and  $OB(c) = \{b,c\}$ . A set that contains the open balls about each of its elements is called an open set, so  $\{a,b,c\}$  is open. Finally, an open set is said to be connected if it cannot be separated into two disjoint open sets, both not empty. Using this definition, we can readily see that  $\{a,b,c\}$  is a connected open set (COS). The definition of a COS indicates that it is a reasonable model of

visual object unity, given that the elements with which we are working must be discrete.

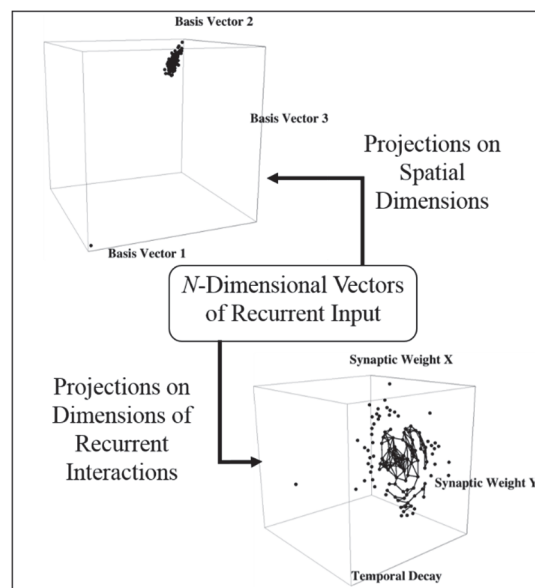


Figure 1: A schematic of the central idea motivating the present work is shown. See text for details.

The work reported here is based on the idea that recurrent neural network inputs are structured by retinal image input, the network's synaptic architecture, the dynamics of synaptic events, and a tolerance relation  $\tau$  into a COS, and thereby "make sense" as visual object unity. It is assumed that recurrent inputs from two network neurons belong to  $\tau$  if they are sufficiently similar as to have indistinguishable effects on network neurons.

Figure 1 is a schematic illustration of recurrent inputs arising from the  $N$  neurons in a network. In a fully-connected network, each neuron contributes  $N$  such inputs that are modelled as an  $N$ -dimensional vector. These vectors can be projected on basis vectors for the 3D space in which the neurons are located. The top left graphic in Figure 1 demonstrates the result for a network with  $N = 1089$  in which the neurons receive inputs from the image of a square. Neurons that receive little input from the image produce very small vectors of recurrent inputs that project to the origin of the coordinate system being used. More active neurons have larger projections, but these provide no information regarding the presence of a unified object.

The bottom right graphic shows projections of the same vectors of recurrent input on a dimension that reflects the rapid decay of recurrent input synaptic conductance with time, and on two dimensions that reflect the decay of recurrent input synaptic

conductance with distance between source and target neurons. Large projections on the temporal decay dimension are produced by neurons that receive retinotopic input from the square image and have recently fired action potentials (APs), and pairs of projections that are joined by line segments form a COS that models visual object unity. It is proposed that, rather than *computing* topological properties, such a network *creates* the perceived unity of a visual object.

The remainder of this paper shows how this idea can be realized in a simple recurrent neural network (RNN). Section 2 provides a description of the network model. Previous work employing singular value decomposition (SVD) of a matrix of recurrent excitatory conductance values  $G(t)$  showed that a small number of basis vectors span the row space of  $G(t)$  and allow a portrayal of stable structures that form in response to an input image (Pavloski, 2011). Section 2.1 shows that the row space basis vectors arise from the distribution of synaptic weights and the decay of conductance values over time. In Section 2.2, evidence for a tolerance relation containing pairs of similar vectors of recurrent conductance values is presented. Simulations show that this tolerance relation permits a COS of the vectors of sodium conductance values produced by active RNN neurons to emerge from the retinal image of an object. Results showing that COSs demonstrate several characteristics of vision are described in Section 2.3. These include just noticeable differences, the Gestalt phenomenon of grouping by proximity, similarities to V1 fMRI data for real motion and apparent motion, and object constancy over rotation and changes of size and orientation of an image. The issue of determining whether a COS is an emergent entity is considered briefly in Section 3. Two approaches to testing the hypothesis that a COS is an objective signature of a unified visual object are described in Section 4, and conclusions are stated in Section 5.

## 2 A RNN THAT PRODUCES CONNECTED OPEN SETS OF CONDUCTANCE VECTORS

Simulated grayscale images were presented to a simulated retina consisting of a 33 x 33 lattice of model neurons. The inputs from the simulated image to these model neurons were arranged so that each receptive field was concentric, with a small diameter ON center within which illumination excites the cell, and a larger diameter OFF surround within which

illumination inhibits the cell. This was done in the following way for each retinal neuron. The membrane potential ( $E_m$ ) was set to 2.5 times the sum of the illumination at each point in the image multiplied by the value of a normal pdf (mean  $\mu = 0$  and standard deviation  $\sigma = 1$ ) at the Euclidean distance between the image point and the location of the neuron, minus .6 times the sum of the illumination at each point in the image multiplied by the value of a normal pdf ( $\mu = 0$  and  $\sigma = 4$ ) at the Euclidean distance between the image point and the location of the neuron. Using this method,  $E_m$  is affected by light in the simulated images as shown in the top left panel of Figure 2. The probability of an AP increased monotonically with  $E_m$  above a threshold.

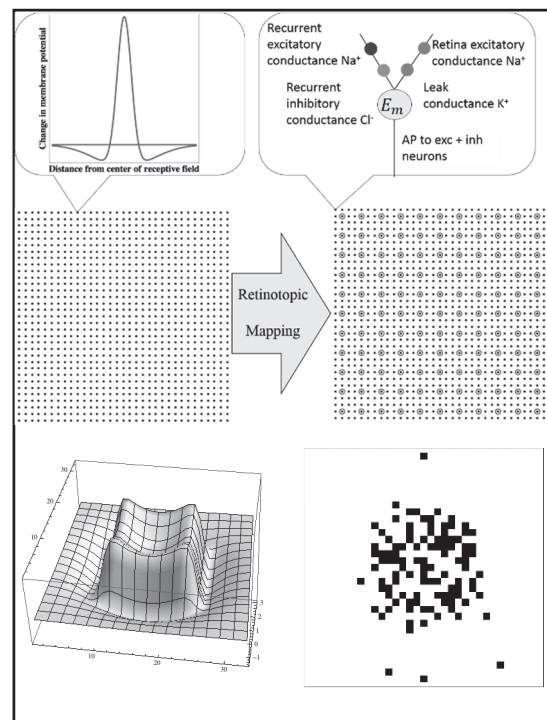


Figure 2: ON-center, OFF-surround neurons and RNN neurons are depicted in the top and middle panels. A retinal response to a 15 x 15 pixel image and a snapshot of RNN excitatory neuron action potentials (APs) are shown in the bottom panel.

Retinal neuron APs map retinotopically to excitatory synapses on excitatory single compartment model RNN neurons, which are also arranged in a 33 x 33 lattice and shown in Figure 2 as dots. An AP produced by any retinal neuron is assigned the value 1 (present) or 0 (absent), and the effect on any excitatory RNN neuron is given by this value multiplied by a synaptic weight, which is .01 times the value of a normal pdf ( $\mu = 0$  and  $\sigma = .03$ ) at the

Euclidean distance between the 2-dimensional location of the retinal neuron and the 2-dimensional location of the excitatory RNN neuron. The summed effects of all retinal inputs on each neuron affected excitatory sodium conductance according to an alpha function (Sterratt et al., 2011); specifically, the value of the conductance on each iteration of the network was set to 0.7 times the summed weighted inputs plus 0.3 times the current value of the conductance.

Each excitatory RNN neuron sends output to all excitatory neurons and also to inhibitory neurons (shown in Figure 2 as circles) that are interspersed among the excitatory neurons in an 11 x 11 lattice. The inhibitory neurons, in turn, send outputs to all excitatory neurons. All synaptic weights decrease exponentially with distance (plus a random component) between the source and target neurons, with inhibition following off less rapidly than excitation. The exponential functions were chosen to promote very stable network dynamics. Excitatory weights vary from a minimum of 0.15 to a maximum of 0.23, and inhibitory weights vary from a minimum of 0.34 to a maximum of 0.37 over the range of distances in the lattice of neurons (distances range from 0. to  $(2 \times 32^2)^{1/2}$ ).

Conductance based equations for the point neurons follow standard sources (Sterratt et al., 2011), and parameter values are taken from O'Reilly and Munakata (2000). Both excitatory (sodium) and inhibitory (chloride) conductance values produced by RNN neuron APs were calculated in the same fashion as the excitatory conductance values produced by retinal neurons. The value of  $E_m$  of each neuron was determined by treating the membrane as an RC circuit with time constant .2 and each synapse as a variable conductance in series with the appropriate equilibrium potential. All synapses were in parallel with each other and with the resting  $E_m$  and leak conductance. Values were scaled so that  $E_m$  varied between 0 and 1. An AP was produced with a low probability (.01) if  $E_m$  is less than a threshold value = .25, and the probability of an AP increased monotonically for  $E_m > .25$ . Updating was synchronous, with every value in the RNN updated on each iteration of the simulation using values of current inputs and values of network variables from the previous iteration. Retinal neuron membrane potentials and APs produced by RNN excitatory neurons on one iteration in response to a 15x15 pixel image are shown in the bottom panel of Figure 2.

## 2.1 Singular Value Decomposition of the Recurrent Excitatory Conductance Matrix

After approximately 11 iterations, the RNN achieves a stable response to an image. As indicated in Section 1, previous work demonstrated that a small number of dimensions describe the row space of  $G(t)$ . The entry in the  $i^{th}$  row and  $j^{th}$  column of this matrix is the conductance value  $g_{ij}$  produced in excitatory neuron  $j$  by excitatory neuron  $i$ . Thus, row  $i$  is vector  $\mathbf{g}_i$  of conductance values in all RNN excitatory neurons produced by neuron  $i$ . SVD of  $G(t)$  reveals that the first three singular vectors serve as basis vectors for the row space of  $G(t)$ , accounting for over 99% of the variance in the entries of the matrix. The top panel of Figure 3 shows row projections on the basis vectors for a COS that results from an 11 x 11 pixel input image on one iteration of the simulation.

The log of the projections of conductance vectors on the first basis vector are linearly dependent on the time of the most recent AP ( $r^2 > 0.99$ ). This is expected because each conductance falls off exponentially over time following the most recent AP. The projections of each conductance vector on the second and third singular vectors are linearly related to the relative row and column position of the neuron giving rise to that conductance vector. It is not possible to quantify the goodness of fit with a single correlation coefficient because the slope of the best-fit line is much smaller for smaller conductance values that are produced by APs occurring in the past. This is illustrated by the middle and bottom panels of Figure 3, which show projections of conductance vectors plotted as functions of each neuron's row position in the lattice shown in Figure 2. For simplicity, axes of all subsequent plots of COSs will continue to be labelled as Row Basis Vectors.

## 2.2 Connected Open Sets of Vectors of Conductances Result from Tolerance to Small Differences in Recurrent Inputs

It is easy to recognize a natural source of tolerance in the RNN. Adjacent excitatory neurons are very likely to receive virtually identical inputs from retinal neurons and from other RNN neurons. They are therefore likely to fire very similar trains of APs and thus to produce very similar vectors of conductance values. This is confirmed by simulations. For example, closely positioned neurons that recently fired an AP in response to a 7 x 7 image yield a mean difference between conductance vector magnitudes

equal to  $5.05 \times 10^{-6}$  ( $se = 2.23 \times 10^{-7}$ ) and a mean difference in angular orientations of  $.03$  rad ( $se = 4.46 \times 10^{-4}$ ). Such small differences in conductance vector magnitudes and orientations are of no consequence with respect to their impact on the temporal evolution of conductance vectors.

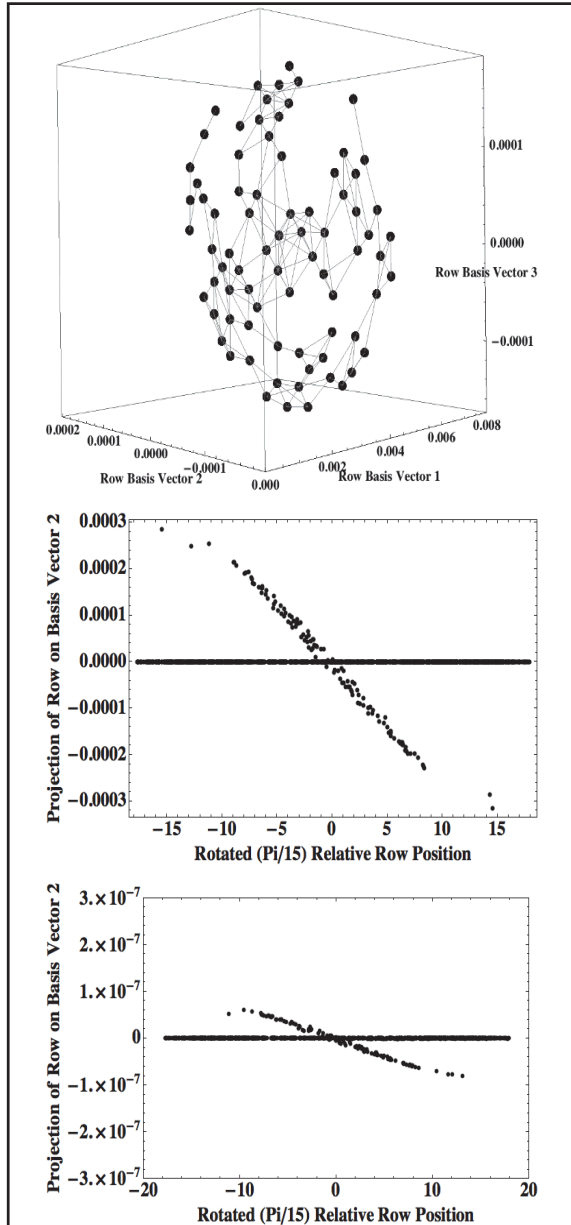


Figure 3: Plot of COS conductance vector projections on three dominant singular vectors (top). Vectors within a tolerance are joined by lines. The projection of each conductance vector on the second singular vector is linearly related to the rotated row position of the neuron giving rise to that conductance vector with a slope determined by the time of the most recent AP (middle, bottom). See Sections 2.1 and 2.2 for details.

Frequency histograms of vector magnitude differences and orientation differences imply that a magnitude difference less than  $10^{-4}$  and an orientation difference less than  $.03$  rad are appropriate criteria for a pair of vectors to belong to the tolerance relation.

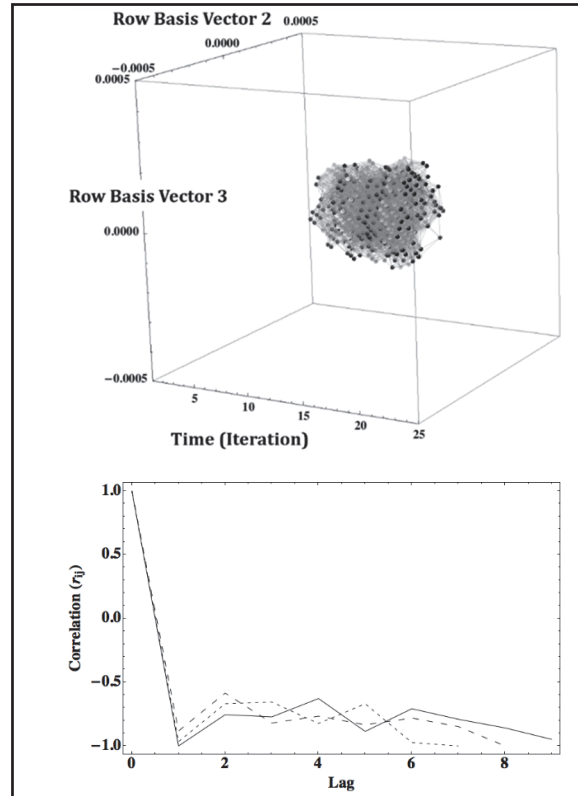


Figure 4: A COS occurs on iterations 11-20 in response to an  $11 \times 11$  input image presented on iterations 6-15 (top). Projections of conductance vectors on the second and third basis vectors for the rows of conductance matrix  $G(t)$  are shown as a function of iteration number. Conductance vectors on successive iterations that are within a tolerance are joined by light gray line segments. No lines are drawn between vectors within a tolerance on a given iteration for this and subsequent figures. The solid curve in the bottom graph plots the function  $r_{ij}$  for iteration  $i=11$  of the simulation, the dashed curve plots results for  $i=12$ , and the dotted curve plots results for  $i=13$ .  $Lag = t_j - t_i$ .

The top panel of Figure 4 plots the COSs that arise from an  $11 \times 11$  pixel input image. The image was shown on iterations 6-15, and COSs appear on iterations 11-20. In this figure, the iteration number is used as the x-axis, and the second and third singular vectors are used for y and z as they were in Figure 3. Conductance vectors on successive iterations that meet tolerance criteria are joined by gray line segments. The spatiotemporal consistency in COS composition occurs jointly with large fluctuations in neurons giving rise to vectors in the COS. This is

demonstrated by the bottom panel, which plots the simple correlation function

$$r_{ij} = (N_{ij} - N_i - N_j) / D_{ij} \quad (1)$$

where  $N_{ij}$  is the number of distinct pairs of neurons giving rise to conductance vectors within a tolerance (tolerance pairs) at times  $t_i$  and  $t_j$ ,  $N_i$  is the number of tolerance pairs that are present at time  $t_i$  but not at time  $t_j$ ,  $N_j$  is the number of tolerance pairs that are present at time  $t_j$  but not at time  $t_i$ , and  $D_{ij}$  is the total number of distinct tolerance pairs present at time  $t_i$  or at time  $t_j$ . The majority of tolerance pairs occurred only once or twice over the 10 iterations of the network for which the correlation function is plotted in Figure 4. Thus, similar conductance vectors are produced on sequential iterations by different pairs of neurons.

### 2.3 COS Phenomena Mimic Visual Phenomena

COSs demonstrate just noticeable differences (jnd's) and grouping by proximity. These phenomena are demonstrated by simulation results depicted in Figure 5. The COSs are shown after the RNN has stabilized (i.e., beginning on iteration 12).

It has been shown that fMRI data from human primary visual cortex (V1) show a moving pattern of activation during perception of real motion and apparent motion (Larsen et al., 2006). It is of interest that the COSs that emerge from the smooth motion of an image and from simulation of the conditions for apparent motion behave very similarly to V1 fMRI data. The COSs that result from these two conditions over 20 iterations are shown in the top and bottom panels of Figure 6.

In a similar fashion, COSs track the change of orientation of the image of a rectangle, a change of size of a square, and rotation of a rectangle, as shown in Figure 7. The behaviour of the COSs mimics object constancy over similar changes in object images.

### 3 IS A COS IN RECURRENT NETWORK INPUTS A MODEL OF LARGE-SCALE ORDER?

Results presented in Section 2.2 demonstrate that similar pairs of conductance vectors that are elements of a COS are produced by different pairs of neurons on sequential iterations of the simulated RNN.

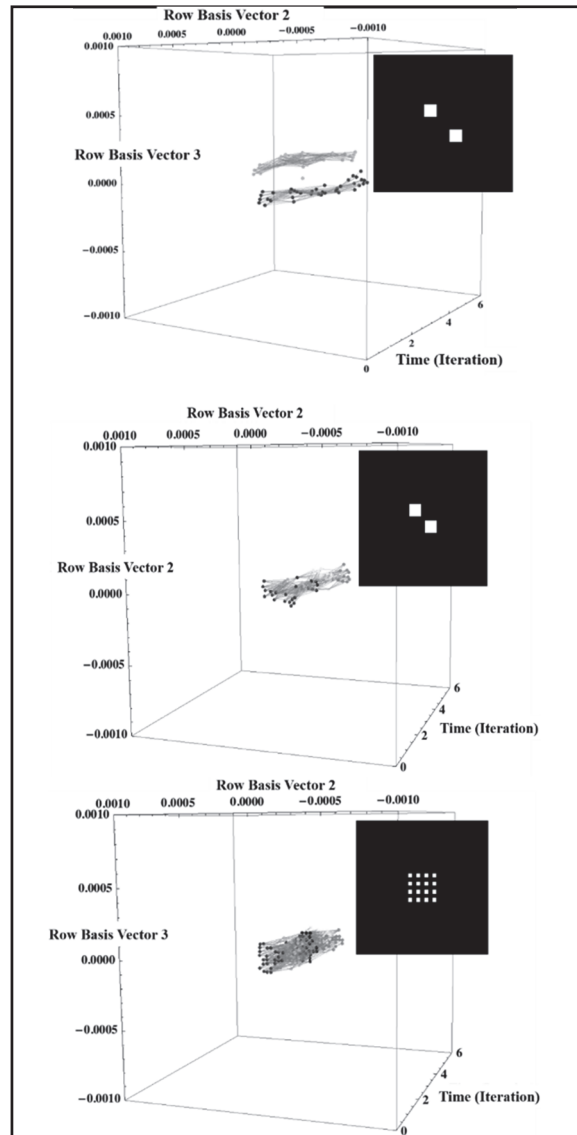


Figure 5: Two COSs emerge in response to two, 3x3 pixel images that are separated by three pixels diagonally (top). One COS emerges when the diagonal separation is reduced to one pixel (middle). Grouping by proximity results in one COS to an image of 16 one-pixel elements with one-pixel spacings (bottom).

This finding suggests the possibility that a COS models emergent large-scale order that is invariant over participating neurons. COS phenomena that mimic visual phenomena (Section 2.3) are consistent with this possibility. For example, a single COS persists over time even as size and orientation of an image change, and a COS persists under the conditions of apparent motion, which involve brief elimination of the image of an object.

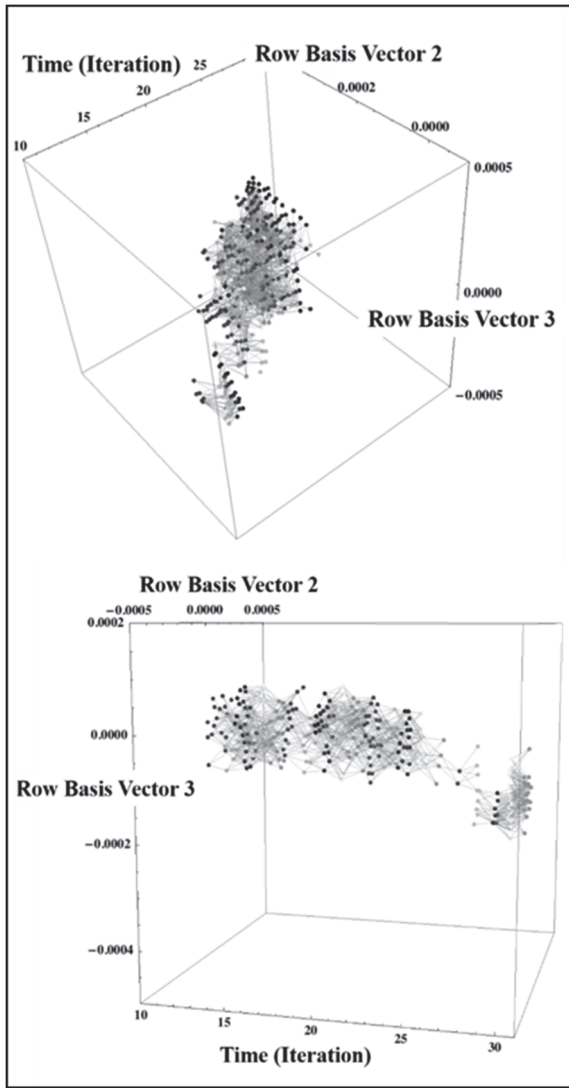


Figure 6: The COSs in the top panel on iterations 11-30 result from an 11 x 11 image shown in one corner for 10 iterations, then shown displaced by 5 pixels horizontally and vertically for 5 iterations repeatedly until finishing at the diagonally opposite corner for 5 iterations. The COSs in the bottom panel shown on iterations 11-30 result from a 5 x 7 image shown in one position for 20 iterations, then not shown for 2 iterations. Each point is then displaced vertically by 9 pixels and shown for 10 iterations.

These results should be replicated using a much larger scale simulation that would include arrangements of a retina and RNN with receptive fields that overlap like those in mammalian visual systems. This would permit the use of more realistic images of multiple objects and should also enhance the similarities in recurrent inputs between adjacent neurons. In addition, asynchronous updating using very small time steps would more closely

approximate biological vision and should enhance the temporal persistence of COSs.

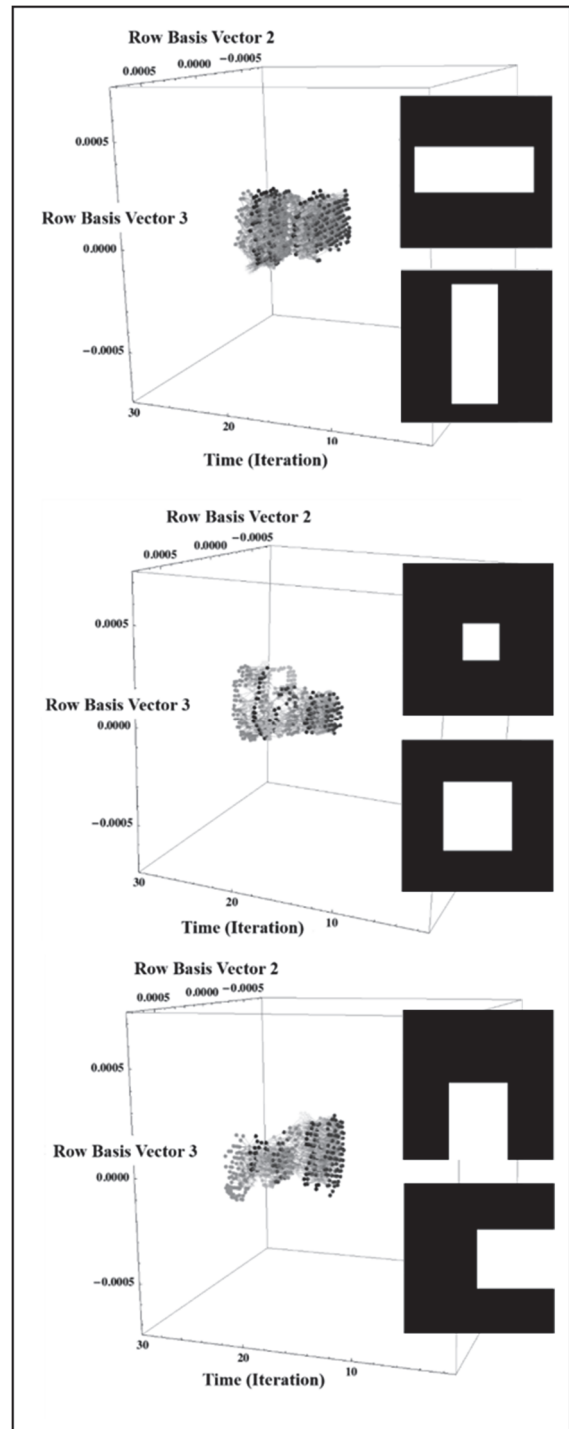


Figure 7: COSs smoothly track step changes in orientation (top) and in size (middle), and a step rotation (bottom). The top image of each pair was shown for 15 iterations and replaced by the bottom image for 15 iterations, and the COSs are plotted from iterations 16-30.

A network with these characteristics should make it possible to analyse the projections of  $G(t)$  on row basis vectors for the presence of topological properties such as the number of connected objects and the number of holes. Such work would provide an approach that would complement the direct introduction of a tolerance relation, as done here.

Two strategies might then be followed in testing the hypothesis that large-scale topological objects emerge within recurrent interactions. The first is to use simulations in order to determine if a COS possesses typically-observed properties of such large-scale order. We expect to find a control parameter that can be varied to modulate the shape of a potential that is a function of an order parameter, such as the density of a COS (e.g., number of conductance vectors per unit volume). Using data gathered from human participants (see Section 4), we will attempt to find a potential function empirically, and to incorporate this in simulations in order to make predictions that can then be tested with human participants.

A second strategy involves implementing a RNN in an electronic circuit. In principle, it should be possible to interface an analog electronic RNN with a biological visual system so that they cooperate to produce one or more COSs. Such an arrangement could serve both as a critical test of ideas that underlie the approach to the hard problem that is advocated, and as a prototype for a prosthetic device. There is no question that many difficult obstacles must be overcome for this strategy to become feasible. Poon and Zhou (2011) provide a fairly recent overview of the challenges and opportunities presented by neuromorphic silicon neurons and large scale neural networks, and a wide-ranging and thorough review of such circuits is provided by Indiveri et al., (2011).

#### **4 IS A COS IN RECURRENT NETWORK INPUTS AN OBJECTIVE SIGNATURE OF PERCEIVED OBJECT UNITY?**

The results presented above are consistent with the hypothesis that a COS of recurrent vectors of sodium ion conductance is an objective signature of perceived object unity. Empirical tests using data collected from human participants and from non-human species are required to test this hypothesis.

Two approaches to devising such tests are considered in this section. The first approach is based on comparisons of dynamical phenomena exhibited by COSs in neural network simulations with

dynamical phenomena in human visual perception. This approach has a strong existing basis in the perception literature, particularly in work based on Haken's (1996) Synergetics. The second approach is much more direct, as it is based on a search for evidence of a COS in recordings of brain activity.

#### **4.1 Do Perceived Object Unity and COSs Exhibit the Same Dynamical Phenomena?**

In addition to the visual phenomena that are mimicked by COSs as presented above, dynamical effects of sequential presentations of stimuli are well documented in perception. For example, categorical perception of speech sounds has been shown to exhibit both enhanced contrast and hysteresis (Tuller et al., 1994). Enhanced contrast occurs when a perception changes from one category to another at one parameter value as values are initially increased and at a higher parameter value as values are subsequently decreased. In hysteresis, the change occurs at a higher parameter value for initial increases than for subsequent decreases. Tuller et al., (1994) showed that the data collected from human participants fit an underlying model for which hysteresis dominates during early trials, and enhanced contrast dominates as experience with the task brings certain cognitive factors into play. The simple RNN has no capacity for such cognitive functions, and is therefore expected to display hysteresis.

The phenomenon of grouping by proximity was used to test this hypothesis. The images used consist of 140 one-pixel spots. One hundred of the spots are repositioned randomly within the 33 x 33 pixel image area on each iteration. The remaining 40 spots are positioned randomly within a square window the sides of which are reduced from a length of 33 pixels to a length of seven over the first 31 iterations; the sides increase over the remaining 30 iterations to the original length of 33. The inset in the top panel of Figure 8 shows images from iterations 1, 10, 20 (top row), 30, 31, 32 (middle row), and 42, 52, and 61 (bottom row). The portion of the graph with forward arrows ( $\rightarrow$ ) plots the size of the emergent COS as the sides of the window containing the critical 40 dots is initially decreased, and the portion of the graph with backward arrows ( $\leftarrow$ ) plots COS size as window size is subsequently decreased. It is clear that hysteresis is present. We are currently testing human participants with a version of the grouping by proximity task that has been modified to make it appropriate for the human visual system. The procedure used by Tuller et al., (1994) for categorical perception of speech

sounds was changed slightly in order to apply it to perception of object unity. In this task, 1600 dots are displayed on each trial. Of these, 1500 are randomly positioned within a 10 x 10 square on each trial. An additional 100 dots are randomly positioned within a square window that grows or shrinks over trials. Dot diameter is 0.2 percent of the width of the 10 x 10 square. The bottom panel of Figure 8 illustrates results from five pilot subjects. On each of two blocks of trials, the length of the sides of the square containing the additional 100 dots was reduced from 10 to 1.5 over the first 100 trials and then increased over the remaining 100 trials to the original length of 10. Hysteresis is present in the total number of reports of a unified object (out of 10 maximum).

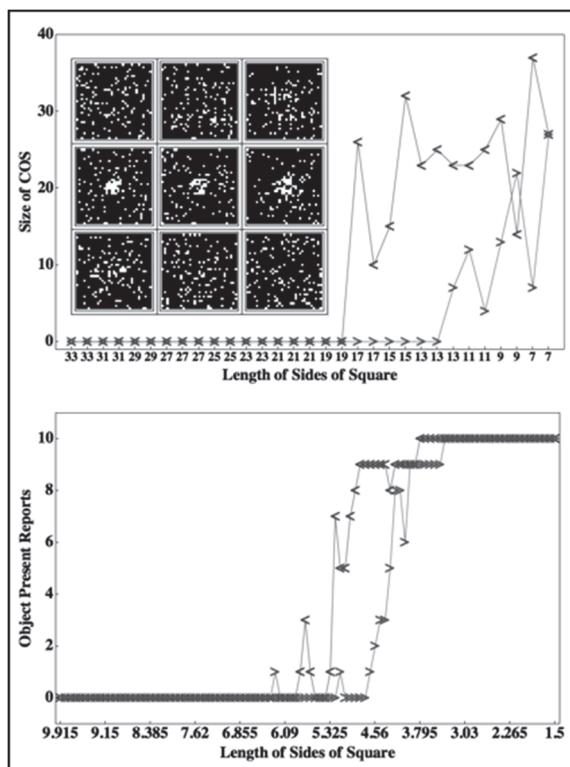


Figure 8: The top panel shows hysteresis in the number of conductance vectors that are elements of a COS. The inset shows simulated retinal images for nine iterations of one simulation, as described in the text. The graph with forward arrows (→) plots the number of conductance vectors in the resulting COS on iterations 1-31, and the graph with backward arrows (←) plots the size of the COS on iterations 32-61. This graph clearly demonstrates hysteresis. The bottom panel shows hysteresis in perception of a unified object for five participants.

## 4.2 Can the Presence of a COS Be Inferred from Recordings of Brain Activity?

A direct test of the hypothesis that a COS of excitatory recurrent conductance vectors is indicative of the experience of visual object unity would be possible if extracranial or intracranial recordings could be used to detect a COS. It is possible that large-scale brain simulations and visualizations (e.g., Jones et al., 2013) could answer this question.

Such large-scale simulations have been shown to model successfully network dynamics of primary visual cortex at multiple scales (e.g., Rangan et al., 2009), and the network model appears to account for V1 activity associated with the line-motion illusion (Rangan et al., 2005). It is important to replicate the strategy used by previous researchers in order to determine if the presence of a COS produces a signature in simulations of recorded activity that include single unit, population, and electroencephalogram recordings and optical imaging with voltage-sensitive dyes. Some of these studies would employ non-invasive methods and can be performed with human participants. Others are clearly invasive and would have to be performed with non-human species.

## 5 CONCLUSIONS

Progress in the development of neurotechnologies is necessarily limited by our current understanding of the specific ways in which neural network activities are involved with particular aspects or qualities of conscious experience. The central problem that we face is theoretical. It is precisely the famous 'hard problem' (Chalmers, 1996; Hut and Shepard, 1996).

The introduction of a formal model of an aspect of experience makes it possible to state a testable hypothesis that bears directly on the hard problem: the unified aspect of a visual object arises as a COS of vectors of recurrent excitatory conductance values emerges from cooperative network activity. Results using a small RNN driven by simulated activity of retinal neurons with a concentric receptive field organization are very promising. These results demonstrate a natural source of tolerance that underlies the formation of a COS, and visual phenomena that include just noticeable differences, grouping by proximity, similarities to V1 fMRI activity patterns in response to real and apparent motion, and visual object constancy with changes in size, shape and rotation are all reproduced by COSs.

The COS is also subject to the nonlinear phenomenon of hysteresis that characterizes multistability in perception.

It is important to use a variety of strategies to test two hypotheses that arise from the work reported here: (1) a COS of excitatory recurrent conductance vectors is a model of large-scale order within recurrent network interactions; and (2) such a COS is an objective signature of the unity or oneness aspect of a visual object.

## ACKNOWLEDGEMENTS

The author wishes to thank Dr. Charles Lamb of the IUP Department of Mathematics for the many positive contributions that he has made to the work reported here in our numerous discussions. The author also thanks Mr. Ian Bright who collected the pilot data reported in Section 4.1 and who contributed in all aspects of that work. Two anonymous reviewers are also thanked for their thoughtful and useful comments.

## REFERENCES

- Block, N. (2001). Paradox and cross purposes in recent work on consciousness. *Cognition*, 79, 347-357.
- Block, N. (2007). Consciousness, accessibility, and the mesh between psychology and neuroscience. *Behavioral and Brain Sciences*, 30, 481-499.
- Chalmers, D. J. (1996). *The conscious mind: In search of a fundamental theory*. New York, NY: Oxford University Press.
- Chen, L. (2005). The topological approach to perceptual organization. *Visual Cognition*, 12(4), 553-637.
- Dehaene, S. (2014). *Consciousness and the brain: Deciphering how the brain codes our thoughts*. New York, NY: Penguin Books.
- Edelman, G. M., Gally, J. A., Baars, B. J. (2011). Biology of consciousness. *Frontiers in Psychology*, doi: 10.3389/fpsyg.2011.00004.
- Haken, H. (1996). *Principles of brain functioning: A synergetic approach to brain activity, behavior and cognition*. New York, NY: Springer.
- Huang, Y., Huang, K., Tan, T., Tao, D. (2010). A novel visual organization based on topological perception. *Computer vision – ACCV 2009. Lecture notes in computer science, Volume 5994*, 180-189.
- Hut, P., Shepard, R. N. (1996). Turning ‘the hard problem’ upside down & sideways. *Journal of Consciousness Studies*, 3, 313-329.
- Indiveri G., Linares-Barranco B., Hamilton T.J., van Schaik A., Etienne- Cummings R., Delbruck T., Liu S-C., Dudek P., Häfliger P., Renaud S., Schemmel J., Cauwenberghs G., Arthur J., Hynna K., Folowosele F., Saïghi S., Serrano- Gotarredona T., Wijekoon J., Wang Y. Boahen K. (2011). Neuromorphic silicon neuron circuits. *Frontiers in Neuroscience*, 5:73. doi: 10.3389/fnins.2011.00073.
- Jones, A., Cardoza, J., Liu, D. J., Jayet Bray, L. C., Dascalu, S. M., Louis, S. J., Harris Jr., F. C. (2013). A novel 3D visualization tool for large-scale neural networks. *BMC Neuroscience* 2013, 14 (Suppl 1):P158
- Larsen, A., Madsen, K. H., Lund, T.E., Bundesen, C. (2006). Images of illusory motion in primary visual cortex. *Journal of Cognitive Neuroscience*, 18(7), 1174-1180.
- Minsky, M. L., Papert, S. A. (1998). *Perceptrons: An introduction to computational geometry (Expanded edition)*. Cambridge, MA: MIT Press.
- O’Reilly, R. C., Munakata, Y. (2000). *Computational explorations in cognitive neuroscience: Understanding the mind by simulating the brain*. Cambridge, MA: MIT Press.
- Pavloski, R. (2011). Learning how to get from properties of perception to those of the neural substrate and back: An ongoing task of Gestalt Psychology. *Humana.Mente Journal of Philosophical Studies*, 17, 69-94.
- Peters, J. F., Wasilewski, P. (2012). Tolerance spaces: Origins, theoretical aspects and applications. *Information Sciences*, 195, 211-225.
- Pomerantz, J. R. (2003). Wholes, holes, and basic features in vision. *Trends in Cognitive Sciences*, 7(11), 471-473.
- Poon, C.-S., Zhou, K. (2011). Neuromorphic silicon neurons and large-scale neural networks: Challenges and opportunities. *Frontiers in Neuroscience*, 5:108. doi: 10.3389/fnins.2011.00108.
- Rangan, A. V., Cai, D., McLaughlin, D. W. (2005). Modeling the spatiotemporal cortical activity associated with the line-motion illusion in primary visual cortex. *Proceedings of the National Academy of Sciences*, 102(52), 18793-18800.
- Rangan, A. V., Tao, L., Kovacic, G., Cai, D. (2009). Multiscale modeling of the primary visual cortex. *IEEE Engineering in Medicine and Biology Magazine*, May 2009, 19-24.
- Roelfsema, P. R. Houtkamp, R. (2011). Incremental grouping of image elements in vision. *Attention Perception & Psychophysics*, 73, 2542-2572.
- Sterratt, D., Graham, B., Gillies, A., Willshaw, D. (2011). *Principles of computational modelling in neuroscience*. New York, NY: Oxford University Press.
- Tuller, B., Case, P., Ding, M., Kelso, J.A.S. (1994). The nonlinear dynamics of speech categorization. *Journal of Experimental Psychology: Human Perception and Performance*, 20(1), 3-16.
- Zhang, J. (2005). Object oneness: The essence of the topological approach to perception. *Visual Cognition*, 12(4), 683-690.